EasyChair Preprint

№ 7120

Deep Rejoining Model for Oracle Bone Fragment Images

Zhan Zhang, Yun-Tian Wang, Bang Li, An Guo and Cheng-Lin Liu

December 1, 2021

Deep Rejoining Model for Oracle Bone Fragment Images

Zhan Zhang[1,2], Yun-Tian Wang[1], Bang Li[1], An Guo[1], Cheng-Lin Liu[2]

[1] Key Laboratory of Oracle Bone Inscription Information Processing, Ministry of Education, Anyang 455000, Henan province, China;
[2] National Laboratory of Pattern Recognition, Institute of Automation of Chinese Academy of Sciences, Beijing 100190, China;
zhangzhan161@mails.ucas.ac.cn

Abstract. Image based object fragments rejoining can avoid touching and damaging objects, and be applied to recover fragments of oracle bones, artifacts, paper money, calligraphy and painting files. However, traditional methods are insufficient in terms of judging whether two images' texture are rejoinable. In this paper, we propose a deep rejoining model (DRM) for automatic rejoining of oracle bone fragment images. In our model, an edge equal distance rejoining method (EEDR) is used to locate the matching position of the edges of two fragment images and crop the target area image (TAI), then a convolution neural network (CNN) is used to evaluate the similarity of texture in TAI. To improve the performance of similarity evaluation, a maximum similarity pooling (MSP) layer is proposed in CNN, and the fully connected layer outputs the two-class probability of whether the rejoining is eligible or not. Our experiments show that DRM achieved state-of-the-arts performance in rejoining oracle bone fragment images and has stronger adaptability.

Keywords: Oracle Bone Fragment Image Rejoining, Deep Rejoining Model, Edge Equal Distance Rejoining Method, Maximum Similarity Pooling

1 Introduction

Object fragments can be rejoined by image analysis to avoid touching or damaging to them. This technology can be used to recover fragments of oracle bones, artifacts, paper money, calligraphy and painting files. There have been many oracle bone fragments found in the history, and the rejoining of them is important for archeology. Traditional methods, mostly based on heuristic rules and hand-crafted features, are human laborious and insufficient in performance, because oracle bone fragments are highly variable in bone size, texture, character size and position [1,2]. Usually, a segment of edge of the source fragment image and that of the target fragment image are selected by exhaustive search to be matched for rejoining [3], and to judge the similarity of texture of the image pair is non-trivial. To search for the pair of edge segments, angle and chain code features in multi-scale image space have been extracted for matching [4]. The ratio of the gap between the boundaries of two fragment images has also been used [5]. The traditional methods [1-5] are insufficient in terms of accuracy, discrimination and adaptability, so they cannot satisfy the need of large-scale rejoining of oracle bone fragments. The keypoint extraction techniques

in computer vision (such as [6-9]) are useful for matching images. But for oracle bone fragments rejoining, since two fragments are complementary in space with no overlap, such keypoints are not helpful for rejoining. Edge and corner based rejoining methods [3-5] would search more incorrect image pairs of oracle bone fragment, because it can not evaluate the texture similarity of image pairs, it is the challenges brought by rejoining oracle bone fragment (see Fig. 1).

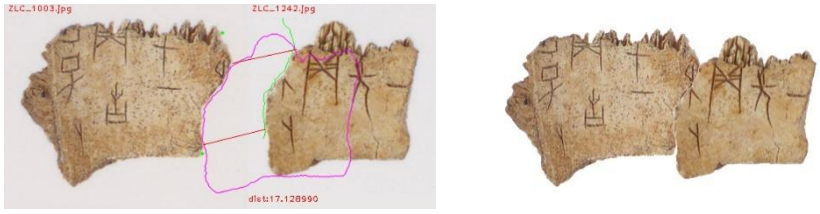

a. Oracle bone fragment images b. Recovering of fragment images

Fig. 1. Oracle bone fragments

Deep learning models (deep neural networks, DNNs) have been widely used in computer vision tasks including object detection, classification and verification. To use DNNs for oracle bone fragments rejoining, there are two key issues: selection of the regions of two images to be compared, and calculation of similarity of two images in texture (whether two fragments are rejoinable or not). While the former step is accomplished using image processing techniques, the latter can be fulfilled using DNN. DNN models include encoding network (EN) [10,11], regional convolution neural network (R-CNN) [12-15], inception network (GoogleNet) [16-18], VGG network (VGG-Net), YOLO [19] and graph network (GN) [20,21], etc. To apply DNN to fragments rejoining, the fully connected layer needs to be re-designed since the two fragments are not overlapping in space.

This paper proposes a deep rejoining model (DRM) for oracle bone fragments rejoining. The model consists of two components: first, an edge coordinate matching method is used to locate the matching position of two oracle bone fragment images, and the target area image is cropped from the rejoined image to be evaluated by CNN. In the CNN, a max similarity pooling (MSP) layer is designed to calculate the similarity of texture feature in the target area image. The CNN functions as a two-class classifier, outputting the probability measuring whether two oracle bone fragments are compatible in texture or not. In our experiments, the DRM report accuracy of 99.56% and 99.81% on the training set and validation set, respectively. Applying the model to rejoining actual oracle bone fragments in the Lvshun Museum, the model has found 14 pairs of new rejoinable oracle bone fragment images, which were not found by human archeologists. The 14 pairs of images include images of cow bones, tortoise back carapace and tortoise belly carapace. This contributes tremendously to the area of archeology. This indicates that the DRM can be used for rejoining the fragments of tortoise shells, cow bones and other fragments, and is highly adaptable.

The rest of this paper is organized as follows. Section 2 reviews related works. Section 3 describes the proposed deep rejoining model. Section 4 presents experimental results, and Section 5 draws concluding remarks.

2 Related Work

The previous rejoining methods more or less rely on human knowledge or hand-crafted features. The edge-corner matching method evaluates the similarity of two fragment image edges according to the sum of the square of the edge length ratios[22]. This method covers three situations: one corner, multiple corners and three corners (see Fig. 2). Every triplet of adjacent points in the contour of the oracle bone fragment image can be used to calculate an angle[4], and in the case of multi-scale space, the feature vector is composed of the outline angle sequence to be matched with that of the target oracle bone fragment image. If the i-th angle of the source contour feature vector and the j-th angle of the target contour feature vector are equal at a certain scale, the two fragment images can be matched at the scale. This method is not suitable for matching those images whose edge has no corners, however.

On locating the target area of two fragment images to be rejoined, DNN can be considered to evaluate the similarity of the two fragment images. However, since two fragments are not overlapping in space, DNN cannot be used straightforwardly. We thus propose to revise the fully connected layer for fragment images rejoining.

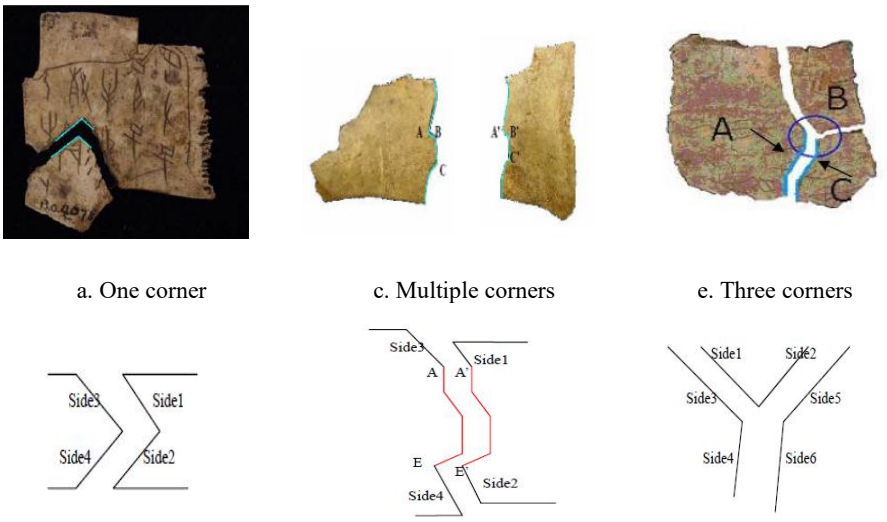

a. One corner c. Multiple corners e. Three corners

b. Two edges d. Multiple edges f. Six edges

Fig. 2. Rejoining of oracle bone fragment images by corner and edge

3 Deep Rejoining Model

In order to solve the above problems, we propose the deep rejoining model to rejoin oracle bone fragment images. Our model consists of two parts: The first part is of a method for matching the edge point coordinates of oracle bone fragment images: an EEDR algorithm is proposed to locate the matching edge position of oracle bone fragment images and crop the target area in the rejoined image that have matching edge segment. The second part is a CNN based model for evaluating oracle bone fragment target area image texture similarity: the ResNet with proposed the maximum similarity pooling (MSP) layer is used to extract the texture features of the target area images, the MSP layer is used to replace the maximum pool layer to calculate the similarity of the texture feature in TAI and improve the accuracy of rejoining oracle bone fragment images. The fully connected layer is used as a two-category model, and to judge whether the oracle bone fragment images are complementary.

3.1 Image Edge Rejoining Method

When extracting the oracle bone fragment image's edge and the edge point coordinates (see Fig. 3a), the green curve is the edge of the source oracle bone fragment image, the pink curve is the edge of the target oracle bone fragment image. Aiming at matching the edge coordinates of oracle bone fragment images, this paper proposes a ways named edge equal distance rejoining method (EEDR), in order to make it easier to understand, firstly we give edge equal pixel rejoining method (EEPR). Generally, when the edge detection algorithm obtains the edge point coordinates, the point on the edge that is closest to the x-axis of the image is taken as the starting point, and the coordinates of the image edge points are achieved counterclockwise along the edge, the edge is stored into a list in form of point coordinate sequence. The downward arrow in Fig. 3a means to extract the coordinates of the image edge in counterclockwise direction. If two images could be rejoined together by their edges, the edge point coordinates in the list of the target image need to be reversed, its direction is shown in the upward arrow in Figure 3a.

3.1.1 Edge Equal Pixel Rejoining Method

As shown in Figure 3a, the image EEPR method will take the midpoint of the local edge of the source image as the center, and rotate the edge of the source image every 2 degrees, the range of the rotating degree is set between [-20,20], so it would obtain 21 rotating edges, they are drawn by the blue curve in Fig. 3a. The translation vector is calculated according to the midpoint of the segment of the source image edge and the segment of the target image edge. The 21 candidate image edges are translated to the edge of the target image and then sampled. As shown in Fig. 3b, in order to reduce the amount of calculation, when acquiring the edge sample points of the source image and the target image, one point is sampled every fixed number of pixels, and the sum of the distances between the corresponding sample points of the source edge and the target edge is calculated as the dissimilarity, and the minimum dissimilarity between

the local edge of the source image and the local edge of the candidate image is used to evaluate whether the local edges of the two oracle bone fragment images can be rejoined. The matching length of two edges is determined by the number of sampling points and the number of pixels between adjacent sampling points, it is generally less than the length of the edges that can be rejoined, the local edge of the source image is equivalent to a sliding window, which is used to match all the local edges of the source image with all the local edges of the target image, and find the position of the smallest distance between the sampling points of the local edges of the two images.

As shown in formula (1), S_j denotes the sampling point at the edge of the source image, j denotes the subscript of the first matching sampling point in the source image edge coordinate sequence, D_i denotes the sampling point at the edge of the target image, and i denotes the subscript of the first matching sample point in the target image edge coordinate sequence. S_{di} denotes the sum of the distance between the sample points of the source image and the target image edge. If the smallest distance between the edge of the candidate image and the edge of the target image is less than the threshold T_d, the local edges of the two images are matching at this location.

3.1.2 Edge Equal Distance Rejoining Method

Since the edges of the image with the same number of pixels may have different lengths, the EEDR method is proposed. As shown in Fig. 3c, when the candidate local matching edge of the source image is rotated and translated to the target image edge, the intersections of the image edge and the circles with the same center and equal distance increasing radius are used as the sampling points, and the sum of the distances between sample points on the edge of the target image and the source image is used as dissimilarity to evaluate whether the two images can be rejoined, the image edge matching length is determined by the number of sampling points and the distance between two adjacent sampling points.

As shown in formula (2), S_{Rj} and D_{Ri} respectively denotes the sampling points of the source image and the target image edges, R_j denotes the subscript of the first matching sampling point in the source image edge coordinate list, and R_i denotes the subscript of the first matching sampling point in the target image edge coordinate list, S_{dRi} denotes the sum of the distances between corresponding sampling points on the edge of the two oracle bone fragment images calculated by the EEDR method, and k represents the number of sampling points. Among the two methods, the EEPR method has a small amount of calculation. Because the EEDR method can skip the missing edge points, and its adaptability is stronger, in the ZLC oracle bone fragment image set, this method finds one pair of matching oracle bone fragment images, their codes are 797 and 799, respectively, as shown in Fig. 3d and Fig. 3e.

$$S_{di} = \sum_{t=0}^{t=k} dist(S_{j+t}, D_{i+t}) < T_d \tag{1}$$

$$S_{dRi} = \sum_{t=0}^{t=k} dist(S_{Rj+t}, D_{Ri+t}) < T_d \quad (2)$$

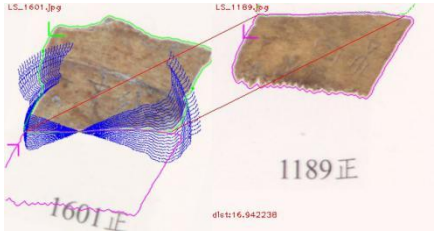

a. Edge direction and rotating edges

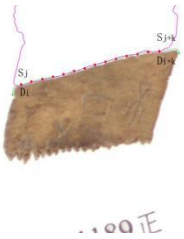

b. Sampling of pixels

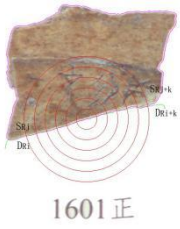

c. Sampling of distance

d. Color images

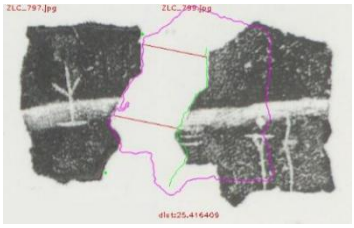

e. Rubbing images

Fig. 3. Edge coordinate matching algorithm

Different scale of oracle bone fragment image need be considered, the resolution of the captured image is usually 300 dots per inch (dpi), 400 dpi or 600 dpi, in order to normalize the texture of the source and target image into the same scale space, we transform the image that has a high resolution into a low resolution. For example, the resolution of image *a* is 300 dpi, and the resolution of image *b* is 600 dpi, we transform the resolution of image *b* into 300 dpi, so image *a* and image *b* would have the same resolution, and image *a* keep its original size, and image *b* would be set to half of its original size.

3.2 Two-Class Model

As shown in the Fig. 4, this paper proposes a deep learning model for rejoining oracle bone fragment images, which includes two parts: EEDR method and ResNet improved by MSP. There are three steps to rejoin the images of oracle bone fragment: (1) Using the EEDR method to find out the matching edge coordinates of two oracle bone fragment images. (2) Rejoining the images who's edge coordinates are matching into a whole image, and cutting the target area image at the matching position, extracting the target image texture similarity feature by improved residual network. (3) Establishing a two-class classification model to evaluate whether the two fragments are rejoinable or not in terms of texture based on target area image's feature. Its activation function is softmax, its kernel weights are initialized by the glorot uniform initializer, the adaptive moment estimation algorithm is used to optimize the model. As shown in Fig. 4a, the target area in the red box is located by EEDR method, and it is used to crop the TAI, (see Fig. 4b) we use the ResNet50 improved by MSP to extract maximum texture similarity feature from the target area image, and use the FCN to train the target area image set and judge whether the two fragment images can be rejoined or not and to give the classification probability.

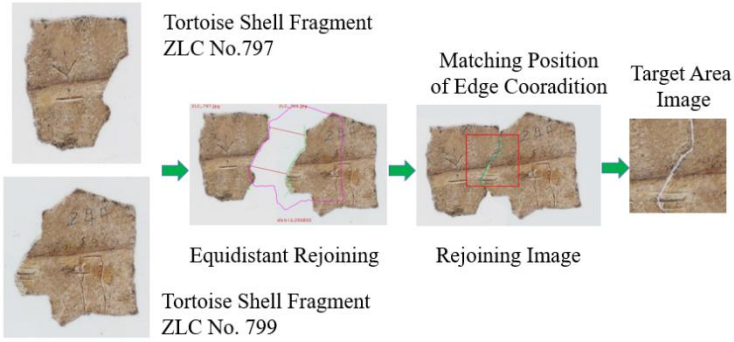

a. Equidistant rejoining method

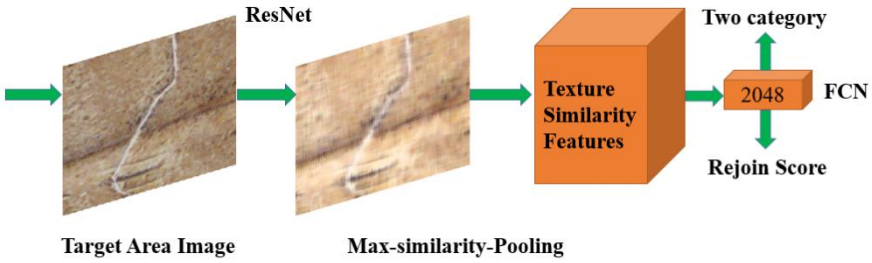

b. Two-class model

Fig. 4. Deep learning model

3.3 Maximum Similarity Pooling

Maximum similarity pooling is proposed to calculate the texture similarity features of target area image[23,24]. After detecting the matching position of the oracle bone images' edges, and cropping the target area image, we would use ResNet to get the convolution residual matrix size of 4x4x2048, and the maximum similarity pooling is proposed to compute the maximum internal texture similarity of the convolution residual image, the result matrix is size of 2x2x2048, and by the operation of maximum similarity pooling, the result matrix would has the similarity relationship and the position information of the pixels in the slip window (Fig. 5), it could increase the discrimination of the convolution feature. Pixel P_0 denotes one pixel in the pooling slip window size of 2x2, and so do P_1, P_2, P_3. $\boldsymbol{\sigma}_{01}$ denotes absolute value of the subtraction between P_0 and P_1, similarly $\boldsymbol{\sigma}_{02}$, $\boldsymbol{\sigma}_{03}$, $\boldsymbol{\sigma}_{12}$, $\boldsymbol{\sigma}_{13}$ and $\boldsymbol{\sigma}_{23}$. The similarity S_{ij} is calculated by formula (3), **a** denotes the harmonized parameter, x denotes product of **a** and $\boldsymbol{\sigma}_{ij}$, the maximum of S_{ij} calculated in the slip window is treated as the maximum similarity pooling value.

$$\boldsymbol{S}_{ij}=\mathbf{e}\text{^}(-1/(\mathbf{a}\times\boldsymbol{\sigma}_{ij})) \tag{3}$$

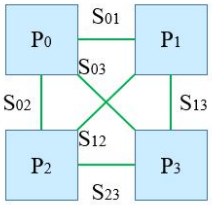

Fig. 5. Maximum similarity pooling

4 Performance Evaluation

4.1 Experiment Dataset

The experiment uses ubuntu operation system, pycharm development environment, tensorflow2.1 framework and opencv3.4 image processing function library. This paper gives a positive and negative sample image set of target area images of oracle bone fragments, the image set includes about 110,000 unrejoinable image samples achieved from the Chinese calendar Tibetan oracle bone fragment image set (ZLC image set) by the EEDR method, and about 20,000 rejoinable image samples achieved by cropping the target area image from BingBian and HuaDong oracle bone fragment image sets, etc. The experiment tests a variety of two classification methods, the training set and the validation set accounted for 80% and 20% of the dataset respectively. In Fig. 6, four rejoinable images size of 121x121 are shown in the first row, and four unrejoinable images size of 121x121 are shown in the second row. When training each model, according to the input image size of ResNet50, the images

are reset to be size of 64x64 or 224*224, each model is trained for twenty epochs to be convergent.

4.2 Performance of Different Methods

The performance of different methods test on the train dataset is shown in table 1, the methods include AlexNet, VGG19, ResNet50, InceptionV3 and MobileNet. The deep rejoining model has the accuracy as 99.56%, it is comparable to other models, and its loss is 0.0023, which is less than other models, but the time it cost is neither higher nor lower than other methods. Test on the validation dataset (see table 2), the model's accuracy is 99.81 and its loss is 0.0078, among all the models the deep rejoining model has the best performance.

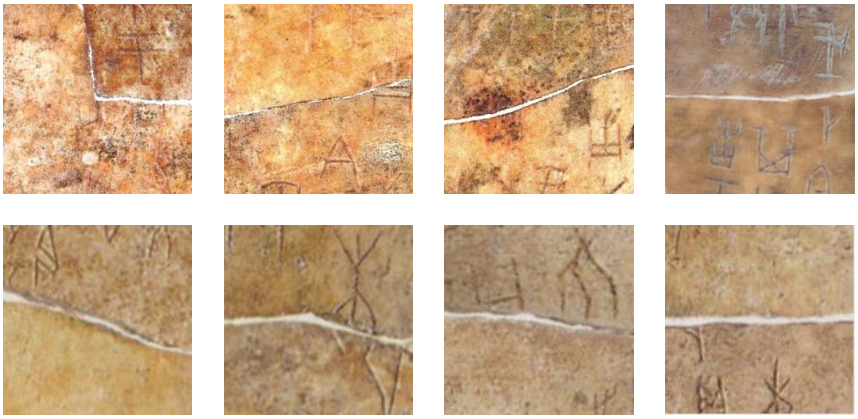

Fig. 6. Rejoinable and unrejoinable images

Table 1. Training accuracy, loss and time (ms/step)

Methods	Accuarcy	Loss	Time
AlexNet	83.39%	0.4489	55
VGG19	83.49%	0.4480	582
ResNet50	99.63%	0.0126	362
InceptionV3	99.68%	0.0112	196
MobileNet	99.68%	0.0108	173
DRM	99.56%	0.0023	300

The ZLC image set which has 1920 images and 12 pairs of matching images is used to test the EEDR method and deep rejoining model. Test on the ZLC image set of oracle bones fragments, the EEDR method could find all the 12 pairs of matching images, but it have found more incorrect matching results. See table 3, the performance of DRM test on the ZLC image set, the deep rejoining model performs

best, and it has searched 11 oracle bone fragments image pairs, and the average probability of the correct classification is 94.23%, and it is higher than AlexNet, VGG19, ResNet50 and InceptionV3, even it is not higher than MobileNet, but it shows a comparable precision with MobileNet.

See Table 2, because ResNet50 is improved as the two-class model in the DRM, its maximum pooling layer is replaced by the maximum similarity pooling layer, so the accuracy of the DRM is 4% more than ResNet50, the DRM has a smaller loss among the deep learning models, and it has found more matching images in the practical rejoining job within a higher probability.

Table 2. The validation accuracy and loss

Methods	Accuracy	Loss
AlexNet	83.69%	0.4447
VGG19	83.38%	0.4499
ResNet50	95.66%	3.2104
InceptionV3	62.39%	2.0513
MobileNet	90.90%	0.1598
DRM	99.81%	0.0078

Table 3. Performance of practical rejoining job

Methods	Pairs	Probability
AlexNet	11	83.76%
VGG19	11	83.34%
ResNet50	10	89.07%
InceptionV3	8	66.29%
MobileNet	11	96.86%
DRM	11	94.23%

4.3 Practical Rejoining Job

In the practical rejoining job, the oracle bone fragments include shells and bones. Then the model works on the image set of oracle bones fragments in Lvshun Museum, which has 2211 images, the model searches 14 pairs of oracle bone fragment images that can be rejoined and these pairs of oracle bone fragments have not been rejoined by oracle bone expert before. We show the number of the 14 pairs of fragments' images (see table 4), and as can been seen in Fig. 7, Fig. 7a, Fig. 7b and Fig. 7c are three pairs of bones from the LvShun Museum, their numbers are 36 and 71, 884 and 340, 1577 and 1457 respectively, and Fig. 7d, Fig. 7e and Fig. 7f are three pairs of shells from the LvShun Museum, their numbers are 1617 and 1330, 1189 and 1601, 1316 and 443 respectively. The experiment result demonstrates that

the model is not only suitable for rejoining bone fragments images, but also suitable for rejoining shell fragments images, at the same time, it shows that the model is more adaptable than the traditional algorithms, because they have not search matching oracle bone fragments images yet.

The EEDR algorithm could search the matching location to the 14 pairs of oracle bone fragment images, but it searched about 500 more disrejoinable image pairs. In order to evaluate the texture similarity of the fragment image pairs and improve the rejoining accuracy, we train the deep learning models such as AlexNet, VGG19, ResNet50, InceptionV3 and MobileNet on the dataset of rejoinable and disrejoinable image to predict the rejoinable probability of target area image. On the image set of oracle bones fragments in Lvshun Museum, our method can correctly judge whether the target area image of the 14 pairs of oracle bone fragment image is rejoinable, and the rejoining probability of correct classification is 92.1%, but AlexNet, VGG19 and MobileNet has given wrong judgement that the 14 target area images' texture is rejoinable or not, InceptionV3 and ResNet50 has respectively given 5 and 2 pairs of oracle bone images pairs, which is correctly judged.

Table 4. Rejoinable oracle bone fragments searched in Lvshun image set

Image Pairs		Image Pairs	
36	71	1189	1601
120	1308	1199	611
324	1115	1316	443
526	1171	1546	1229
629	765	1577	1457
803	859	1610	1612
884	340	1617	1330

Table 5. Numbers of correct rejoinable image pairs searched by different models

Model	AlexNet	VGG19	ResNet50	InceptionV3	MobileNet	DRM
No.	0	0	2	5	0	14
Prob	--	--	89.67%	79.62%	--	92.10%

5 Conclusions

The deep rejoining model can be used in the practical job to rejoin the oracle bone fragment image, and it has a state-of-the-art performance, and it suitable for rejoining images of oracle bone fragments, ceramic fragments, bamboo slip fragments, ancient books and calligraphy fragments, etc., and also suitable for rejoining images of

banknotes and invoice fragments in the financial field. But when the image include the fracture of the oracle bone in the third dimension, the EEDR method would find an incorrect boundary of the fragment's image, the DRM would not work well. So the future job is to improve the model's effectiveness and increase the accuracy and robustness of rejoining fragment images.

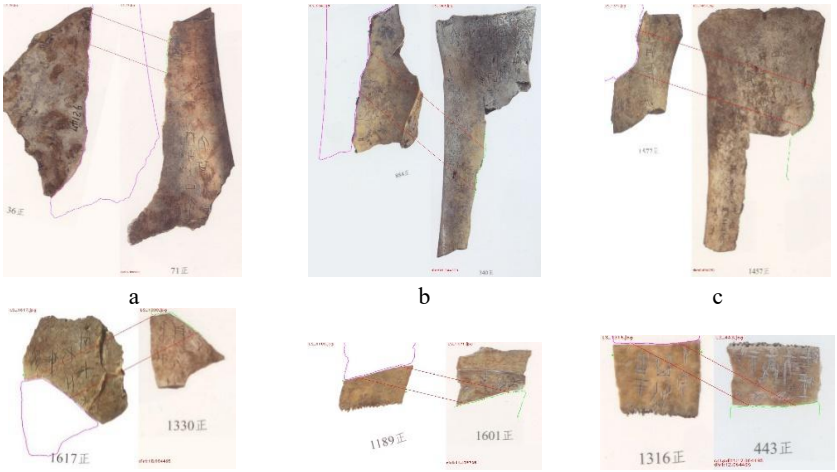

Fig. 7. Pairs of bones and shell fragment images searched

Acknowledgements

This work has been supported by the National Natural Science Foundation of China (62106007, 61806007), Henan Education Department Project (212102310546) and Anyang Normal University Science&Technology Research Project(2021C01GX012).

References

1. Chou H., Opstad Dg.: Computer Matching of Oracle Bone Fragments: A Preliminary Report on a New Research Method. Archaeology, 26(33), 176-181 (1973)
2. Tong E., Zhang S., Cheng J.: Preliminary Report on The Use of Computers to Rejoin Fragments of Shang Daibujia. Journal of Sichuan University (Natural Science Edition), 2, 57-65 (1975)
3. Zhang C., Wang A.: A Computer-Aided Oracle Bone Inscription Rubbing Conjugation Method. Electronic Design Engineering, 20(17), 1-3 (2012)
4. Liu Y., Wang T., Wang J.: The Application of the Technique of 2D Fragments Stitching Based on Outline Feature in Rejoining Oracle Bones. In: International Conference on Multimedia Information Networking and Security, pp. 964-968 (2010)
5. Wang A., Liu G., Ge W., et al.: Oracle Computer-aided Conjugation System Design. Computer Engineering and Applications, 46(21), 59-62 (2010)

6. Tublee E., Rabaud V., Konolige K., Bradski G.: ORB: an efficient alternative to SIFT or SURF. In: IEEE International Conference on Computer Vision. 58(11), 2564-2571 (2011)
7. Leutenegger S., Chli M., Y. Siegwart R.: BRISK: binary robust invariant scalable keypoints. In: IEEE International Conference on Computer Vision. 58(11), 2548-2555 (2012)
8. Alahi A., Ortiz R., Vandergheynst P.: FREAK: fast retina keypoint. In: IEEE Conference on Computer Vision and Pattern Recognition. 157(10), 510-517 (2012)
9. Zhang Z., Yang D., Lian M.: Circumferential Binary Feature Extraction and Matching Search Algorithms. IEEE Signal Processing letters, 25(7), 1074-1078 (2018)
10. Zhang H., Xue J., Dana K.: Deep TEN: Texture Encoding Network. In: IEEE Conference on Computer Vision and Pattern Recognition, pp. 2896-2905(2017)
11. Xue J., Zhang H., Dana K.: Deep Texture Manifold for Ground Terrain Recognition. In: IEEE Conference on Computer Vision and Pattern Recognition, pp. 558-567 (2018)
12. Girshick R., Donahue J., Darrell T., Malik J.: Rich feature hierarchies for accurate object detection and semantic segmentation Tech report. In: IEEE International Conference on Computer Vision, pp. 580-587 (2014)
13. Girshick R.: Fast R-CNN. In: IEEE International Conference on Computer Vision, pp. 1440-1448 (2015)
14. Ren S., He K., Girshick R., Sun J.: Faster R-CNN: Towards Real-time Object Detection with Region Proposal Networks. IEEE Transactions on Pattern Analysis and Machine Intelligence, 39(6), 1137-1149 (2017)
15. He K., Gkioxari G., Dollar P., Girshick R.: Mask R-CNN. IEEE Transactions on Pattern Analysis and Machine Intelligence, 42(2), 386-397 (2020)
16. Szegedy C., Liu W., Jia Y., et al.: A Going Deeper with Convolutions. In: IEEE Conference on Computer Vision and Pattern Recognition, pp.1-9 (2015)
17. Szegedy C., Vanhoucke V., Ioffe S., et al.: Rethinking the Inception Architecture for Computer Vision. In: IEEE Conference on Computer Vision and Pattern Recognition, pp. 2818-2826 (2016)
18. Szegedy C., Ioffe S., Vanhoucke V., Alemi A.: Inception–V4, Inception – ResNet and the Impact of Residual Connections on Learning. In: The 31th AAAI Conference on Artificial Intelligence, pp. 4278-4284, (2016)
19. Redmon J., Divvala S., Girshick R., Farhadi A.: You Only Look Once: Unified, Real-Time Object Detection. In: IEEE Conference on Computer Vision and Pattern Recognition, pp. 779-788 (2016)
20. Ruiz L., Gama F., Marques AG., Ribeiro A.: Invariance-Preserving Localized Activation Functions for Graph Neural Networks. IEEE Transactions on Signal Processing, 68, 127-141 (2020)
21. Cao W., Yan Z., He Z., et al.: A Comprehensive Survey on Geometric Neural Networks. IEEE Access, 8, 35929-35949, (2020)
22. Lin Y.: Exploiting Information Science Technology to Rejoin An-yang Oracle bones/ Shells. Tsinghua University, Taiwan, pp.32-41 (2006)
23. Zhang Z., Yang D.: Internal and External Similarity Aggregation Stereo Matching Algorithm. In: The 11th International Conference on Digital Image Processing, 11179, pp.62, (2019)
24. Mei X., Sun X., Dong W., Wang H., et al.: Segment-tree based cost aggregation for stereo matching. In: IEEE Conference on Computer Vision and Pattern Recognition, pp. 313-320 (2013)